Effect of snow-covered ground albedo on the accuracy of air temperature measurements

Chiara Musacchio[1], Graziano Coppa[1], Gaber Begeš[2], Christina Hofstätter-Mohler[3], Laura Massano[4], Guido Nigrelli[5], Francesca Sanna[6], Andrea Merlone[1]

[1]Istituto Nazionale di Ricerca Metrologica, Strada delle Cacce 91, 10135 Torino, Italy
[2]Univerza v Ljubljani – Laboratorij za Metrologijo in Kakovost, Ljubljana, Slovenia
[3]Bundesamt für Eich- und Vermessungswesen, Wien, Austria
[4]Università degli Studi di Torino, Italy
[5]Istituto di Ricerca per la Protezione Idrogeologica - Consiglio Nazionale delle Ricerche, Torino, Italy
[6]Istituto per le Macchine Agricole e Movimento Terra - Consiglio Nazionale delle Ricerche, Torino, Italy

Correspondence to: Graziano Coppa (g.coppa@inrim.it)

Abstract. Solar radiation is one of the main factors introducing significant deviations between thermometers reading and true air temperature value. Techniques to protect the sensors from direct radiative influence have been adopted almost since the beginning of meteorological observations. Reflected radiation from a snow-covered surface can also cause extra warming to thermometers hosted in solar shields, not always optimized to protect the sensors from this further backward radiative heat transfer. This phenomenon can cause errors in near-surface temperature measurements results, with relevant impact on the quality of data records and series. The study here presented experimentally evaluates the effect of reflected radiation from snow-covered surface, on the accuracy of air temperature measurements. The investigation is based on evaluating temperature differences between pairs of identical instruments positioned above ground covered by natural vegetation, being one in snow-free conditions and the other above snow-covered surface, at the same time and in the same site. The work involved a representative number of sensors and shields, of different typologies, from different manufactures. A mountain site with appropriate field conditions, offering long-lasting snow presence to maximize data availability, was selected to host the experiment. Quantities of influence such as relative humidity, wind speed and direction, solar radiation (direct and reflected) were constantly measured. The main findings of this work showed that none of the involved instruments have been immune from the extra heating due to the snow reflected radiation. Excluding night times and windy days or with low incident radiation, the differences among sensors positioned above natural soil and identical ones exposed to snow albedo, ranged up to more than 3 °C, with larger contribution below 1 °C and still significant amount of data between 1 °C and 2 °C. Solar screens with forced ventilation showed a partially reduced effect, with respect to most of the naturally ventilated ones. Full data analysis is here reported, together with complete results and uncertainties.

1 Introduction

The World Meteorological Organisation (WMO) Commission for Climatology and the Global Climate Observing System (GCOS) are recommending study and definition of measurement methods for reference grade networks, installations, to generate top quality data for meteorology and climate studies (GCOS, 2019). A key requirement for a station taking part in a reference network is a documented traceability and understanding of the total measurement uncertainty (Thorne et al., 2018). Consistent uncertainty calculation needs complete knowledge of the measurement system, the sensors calibration uncertainty, the characteristics of the site and the effects of environmental parameters such as wind, solar radiation and precipitation. Among the numerous observed Essential Climate Variables (ECV), near-surface (1.25-2 m, WMO, (2012)) atmospheric air temperature measurements have been collected for one and a half centuries. Such data series form the basis of scientific knowledge on local and global climate trends (Camuffo and Jones, 2002). Land-based stations are equipped with different kinds of thermometers whose performances have constantly improved. Today, top quality instruments involve platinum resistance sensors and high-level reading and recording electronics. Many efforts have also been made to minimise the effect of quantities of influence on measurement results, with the aim to reduce the associated errors and measurement uncertainty. Solar radiation is one of the main factors influencing the instruments, causing significant deviations between sensors readings and real air temperature. Techniques to protect sensors have been adopted almost since the beginning of meteorological observations. Shields to avoid direct solar radiation reaching the sensing element have been developed, from Stevenson screens (Stevenson, 1864) to modern "pagodas" and naturally or mechanically ventilated solar shields. Recent intercomparisons were organized by WMO (Lacombe et al., 2011) to evaluate the performances and differences among the numerous solutions adopted by manufacturers. While the practical/technical features offered by these shields are now optimized and prescribed (WMO, 2012), their capability to protect the thermometers from backward radiation, reflected by the ground, is rarely evaluated, taken into account in measurements or documented in datasheets. This is dependent on the so called "albedo", indicated with α, which is the ratio of reflected radiation with respect to the global radiation received by the ground that, in case of snow cover, is increased up to 95 % (Barry and Blanken, 2016). Like global radiation, this reflected component can cause extra warming of instruments, introducing errors in near-surface temperature data series, with relevant impact on detected maximum values and anomalies. Such instrumental errors have different magnitudes depending on the equipment, and the technical solutions adopted in manufacturing thermometers and shields. This phenomenon is particularly relevant in monitoring mountain climate, where the duration of snow cover is high (Nigrelli et al., 2018).

Only few studies in literature evaluate the effect of albedo of snow-covered land on temperature sensors: among them, the most significant work is from Huwald et al., (2009) based on a different approach and limited to a single typology of sensor and screen.

The task of the present work is to observe, measure and quantify the effect of extra heating on different kinds of instruments positioned above snow-covered land, in terms of deviations of sensors readings from actual temperature values. This work is the result of a seasonal in-field experiment, following a metrological protocol and experimental method, defined and described

in a previous study (Musacchio et al., 2019). The investigation is addressed at the evaluation of relative difference between the readings of pairs of identical sensors protected by solar shields as provided by manufacturers. One pair is positioned above snow-covered surface, while the other above grass-covered ground, in the same site, at the same time under equal environmental and topoclimatic conditions.

The problem of albedo effect on air temperature instruments can be included as a part of the general study on assessing data quality and uncertainty in near-surface air temperature measurements. This wider subject is now being analysed and discussed by the WMO expert teams of the Infrastructure Commission (INFCOM) and is a key aspect in the creation of the Climate Reference Networks for the Global Climate Observing System (GCOS). The complete knowledge and evaluation of uncertainty budget components on air temperature measurement is also included in the roadmaps of scientific activities of the Working Group for Environment of the *Comité Consultatif de Thermométrie* (CCT - Consultative Committee for Thermometry) of the *Bureau International des Poids et Mesures* (BIPM - International Bureau of Weights and Measure) (CCT, 2017).

The activities here reported have been carried out in the framework of the MeteoMet project (Merlone et al., 2015a, 2015b, 2018), a funded joint research initiative of the European Metrology Research Project (EMRP) grouping a wide consortium of National Institutes of Metrology (NMIs), research institutes, universities and National Meteorological and Hydrological Services (NMHSs).

2 Measurement protocol and experimental method

The experiment here presented follows the prescriptions and assumptions proposed by Musacchio et al., (2019) where a measurement protocol is presented, following a theoretical study on the influence of various parameters such as wind speed and direction, snow cover thickness, incident solar radiation, snow conditions and humidity on air temperature measurements above snow-covered ground. In the cited work, the authors also give guidelines on the experiment design and the evaluation of uncertainty components, as well as laboratory characterisations of instruments and the treatment of all identified quantities of influence, both instrumental and environmental. Based on these considerations, a measurement protocol was prepared for the realization of the field experiment, giving prescriptions on:

- design of the experimental set-up and definition of site requirements;
- evaluation of the quantities of influence;
- sensors characterization in laboratory and in field;
- evaluation of uncertainty components.

2.1 Experimental set-up and site requirements

The "albedo effect" investigated here is defined as is the sensors' overheating due to reflected radiation from snow and it is measured as differences of air temperature readings t_{air} between pairs of identical sensors inside identical shields, one at a point *a*, above snow, the other at a second point *b*, snow-free area: this difference is here indicated as

$$\Delta t_{air} = t_{air}(a) - t_{air}(b) \quad (1)$$

and includes all the corrections evaluated for each pair of sensors during the laboratory and field characterisations, described in the following Sections.

These two measurement points are arranged in close vicinity and on a flat surface, free from obstacles, thus exposed to the same topoclimatic conditions, but far enough to accommodate a significant area covered by snow on one point and a sufficient area (at least 5 m of radius) with natural ground left free from snow on the other point. Readings from each pair of sensors are recorded by means of a single data logger. The investigated effect is therefore the result of a relative analysis of temperature differences, involving identical instruments and single reading unit: this allows for the minimization of influencing factors and uncertainties. Halfway between the two measurement points, other instruments are deployed to measure the quantities of influence, which took part in the analysis as uncertainty components.

Following the experimental protocol described in Musacchio et al., (2019), the site hosting the experiment requires a number of specific features. It must be an open, flat surface of at least 50 m of diameter with a minimum presence of obstacles - as trees, buildings or roads in the surrounding area - and spatially uniform solar exposure during the daytime central hours. Snow must be present for a significant amount of time; underneath it, the ground must be covered with natural low vegetation. Other characteristics are related to logistic aspects such as: electrical power available throughout the winter, easy access for maintenance, no agricultural or sport activities, strictly reduced access to public and no presence of vehicles. The experimental site scheme is described in Fig. 1.

2.2 Quantities of influence

The main quantities of influence on temperature measurements for the evaluation of the albedo effect must be constantly monitored during the experiment. Musacchio et al., (2019) identified wind speed, air relative humidity and solar radiation as major contributors. Global (downward) and reflected (upward) solar radiations were measured in the same position of each temperature sensor to associate temperature differences to radiative budget. Without going into too much detail, which is available in the cited work, other quantities were identified as important, like snow depth and conditions; they influence the albedo effect in terms of functional evaluation, but since this work aims at detecting the maximum value of the effect, they have been monitored (see Sect. 3.2) but excluded from the analysis. Some other quantities, like snow density and solar zenith angle, have been considered but ultimately not monitored: the former, following e.g. Bohren and Beschta, (1979), who concluded that snowpack albedo was only weakly dependent upon it; the latter as well, given the theoretical study of Xiong et al., (2015) who showed that, at high values of albedo like those proper of snow, the dependence on the solar zenith angle is

basically flat; at lower values, the dependence steepens after ~60° which is basically never achieved at our site given its particular orography.

2.3 Sensor characterization

Before starting the experimental activities in the field, temperature sensors have been characterized in order to understand their behaviour in different situations. The experimental protocol prescribes two different characterization phases: in laboratory and in field conditions.

The laboratory characterization is needed to evaluate possible systematic differences between pairs of sensors exposed to the same temperature under controlled conditions. Since the investigation is based only on relative temperature differences among pairs of identical instruments, the sensors calibration is not strictly necessary as no traceable absolute temperature measurements are required for the evaluation of the albedo effect in field. This avoids the inclusion of the calibration uncertainty in the overall uncertainty budget and makes the adoption of this procedure easier, also for users willing to make similar analysis without the calibration costs and time required. Laboratory controlled conditions also allow the evaluation of the sensors' stability, sensitivity and resolution of the readout.

Different systematic biases can arise when the sensors are deployed in the field, due to environmental factors. For this reason, an in-field characterization of the sensors is also needed to evaluate their behaviour in such conditions. Performing an estimation of the uncertainty components of on-site measurements is necessary to quantify the accuracy reached in the experiment. For more details, Musacchio et al., (2019) give an in-depth description of the whole method, as well as its assumptions and prescriptions.

3. Experimental set-up, characterizations of site and instruments, uncertainty components

The experimental activity reported in the present work was carried out in the framework of the MeteoMet project. Pairs of systems composed by different sensors, shields of different shapes and dimensions, mechanically aspirated or naturally ventilated, were lent directly by the manufacturers along with their data loggers in order to have a range of such commonly used devices as broad as possible. In the end, six different pairs of systems from four different producers were selected for the experiment, and labelled from A to F; their main characteristics are described in Table 1.

Additional sensors for the measurement of the quantities of influence were installed, including a cup-and-vane anemometer, a thermo-hygrometer (both positioned in the central measurement point of the experimental area) and two albedometers, one for each measurement point (Table 2). The air temperature measured in the central point is not included in the evaluation of the differences among the pairs of sensors under test, nor it contributes to the uncertainty budget. This further air temperature value is recorded as another potential quantity of influence, in terms of further possible dependence of the temperature differences also on the temperature itself, in addition to the one investigated in laboratory.

3.1 Laboratory tests and characterization

Tests on the selected sensors were performed in laboratory for the characterization of the sensors and the complete system (Fig. 2).

This part of the work was performed in the new "Climate Data Quality Laboratory" of the Istituto di Ricerca per la Protezione Idrogeologica - Consiglio Nazionale delle Ricerche (IRPI-CNR). During this phase, a study of the different data loggers working principles was also made, together with the evaluation of best mounting solutions.

The activities started with an evaluation of the differences between readings by each pair of sensors, without shields, in stable temperature conditions, to check for systematic biases. The sensors were then assembled in the shields and all the temperature measurements differences of each pair of instruments, Δt_{instr}, were measured. The characterization was then performed in a controlled environment with slow temperature change, to keep into account possible effects, without being affected too much by the sensors' dynamics (intended as the behaviour of the sensor exposed to changes in temperature – the time response – as well as to the changes of other influence quantities). Rapid air temperature transients (implying thermodynamic non-equilibrium with the environment), both in the lab and on site, will in fact not be included in the final data analysis, since sensors dynamics can predominantly influence the trueness of the analysis (Burt and de Podesta, 2020). All sensors (except for two pairs, E and F, that joined the experiment later) underwent this laboratory characterisation in order to obtain the information reported in Table 3, along with their uncertainties $u_{\Delta t_{instr}}$ as evaluated in Sect. 3.1.2.

Stability of the instruments was also tested in laboratory during a one-month continuous acquisition, to check for longer term drifts and potential maintenance required in field. No failures or significant effects were observed.

3.1.1 Laboratory

The laboratory controlled experimental conditions have been evaluated in the testing zone, using traceable reference sensors. Room temperature drift was found to be < 0.02 ℃ for one day and < 0.05 ℃ over one week. For time interval corresponding to data loggers' acquisition and recording times (tens of minutes), the laboratory air temperature stability was evaluated as $u_{stab} = 1$ mK.[1]

The temperature homogeneity was measured and found to be < 0.05 ℃ $\cdot$ m^{-1}. Sensors were positioned at a distance of about 20 cm one another, as a compromise between minimizing the gradient and avoiding mutual influences such as heating from the electronics or fan motors. The uncertainty due to the laboratory temperature homogeneity was therefore evaluated as $u_{hom} = 0.01$ ℃.

The total uncertainty contribution due to laboratory conditions was evaluated as $u_{lab} = \sqrt{u_{stab}^2 + u_{hom}^2} = 0.01$ ℃ for all the sensors.

[1] Metrological convention allows for temperature to be expressed in °C and temperature differences in K (BIPM, 2019).

3.1.2 Instruments

The evaluation of possible systematic differences Δt_{instr}, among pairs of identical sensors kept at the same temperature (within the laboratory homogeneity uncertainty) was performed by repeated readings over several intervals of about one hour. As shown in Fig. 3, all sensor pairs were found to have systematic differences Δt_{instr}, which have to be taken into account for the correction of field data. Associated uncertainty values are reported in Table 3. The repeatability of temperature differences Δt_{instr} contribute to the uncertainty budget with a component reported as $u_{\Delta t_{instr}}$.

Finally, a check for possible sensor drifts was performed after the field campaign and exposure to meteorological conditions. In particular, the drift of Δt_{instr} was evaluated again in stable laboratory conditions. The drift was then evaluated as differences in the systematic differences measured before and after the field campaign: values were found to be of the same order of magnitude of the instruments noise. This is an expected result, since only high-performance temperature sensors have been selected, normally produced to guarantee top level stability in time and low drifts, to reduce maintenance and recalibrations by the users. The drift in the relative difference becomes therefore negligible for the duration of the experiment and no correction or uncertainty components have been included.

3.2 Measurement site and experiment set-up

Since a significant snow cover was needed for the experiment, a mountain site in the Alps was chosen, to assure the presence of snow cover throughout the winter.

The measurement site, selected to meet logistics and experimental requirements, was found in the municipality of Balme at 1410 m of elevation (45°18’9.31” N, 7°13’19.18” E), in the Ala Valley, northwest of Turin, Italy (Fig. 4).

Only a 3-m-wide local road with almost no traffic and a small unmanned building were present in the area, at more than 50 m from the measuring point. Coppa et al., (2021b) performed a metrological quantification of the influences on air temperature measurements introduced by the proximity of roads, that revealed a significant effect only at closer distances (less than 50 m), mainly at very low or even null values of incident radiation; its presence was therefore considered negligible. According to a similar experiment for the evaluation of the effect of buildings, (Garcia Izquierdo et al., in prep) a building of the size of the hut and at that distance causes no influence in air temperature records. Moreover, during the experiment set-up, great care has been put in order to place both measurement points at similar distances from each possible source of heat and disturbance: their potential influences affect both measurement points in the same way, thus cancelling out during relative differential evaluations.

The chosen area turned out to be a reasonable compromise between the necessity of an alpine location in terms of snow cover presence and duration, and the logistics of an instrumented research site.

The equipment was installed following the protocol described in Musacchio et al., (2019). The experimental scheme of Fig. 1 was followed: the two external poles hosting the pairs of identical shielded thermometers and the albedometers, the central one with the data loggers, the electric power connection and the auxiliary measurements of humidity, wind speed, wind

direction and central air temperature (Fig. 5(a) and 5(b)). The two instruments of each pair were positioned in the same orientation and in case of asymmetric shapes, following manufacturers specifications (i.e., ventilation aperture facing North). After significant precipitation events, the snow was removed from a 5 m radius area centred in point *b* (Fig. 6(a) and (b) respectively show the site before and after the removal of snow); site and instruments were constantly supervised and meteorological conditions recorded. In order to select periods when the albedo effect can be better detected in its maximum values, as defined in the model described in Musacchio et al., (2019), a selection of the ideal meteorological conditions was necessary. The 5 m radius was decided as a compromise between maximising the snow-free area under the sensor and having the measurement points close enough to keep the assumption of homogeneity of local weather conditions. This radius could not be expanded because the third measurement point, i.e., the one carrying control and ancillary measurements, would fall in the snow-free area, while it was important that these measurements were representative of the natural state of the site. This setup limits the albedometer to a footprint of 146°, out of the theoretical 180° (and effective ~170°) it is able to cover; this was deemed acceptable, considering for instance that doubling the snow-free radius would have quadrupled the area to be freed, while merely adding 16° to the footprint. Temperature sensors are much less influenced by the snow-free radius, given that shields have a smaller angle of view.

As mentioned in Sect. 2.2, the experimental protocol mandates an evaluation of snow depth and conditions for a full understanding of the quantities of influence. Instruments have been positioned at 2 m from the ground and during the whole measurement campaign the snow thickness never surpassed 40 cm (measured by a simple ruler), thus keeping sensors at a distance of at least 1.5 m from the surface below (both above natural soil and snow-covered area). In the measurement protocol, a recommendation to remove data in case of snow depth over 1 m was included, to avoid other effects (extra cooling, turbulences) from introducing errors or uncertainties. Observing snow conditions was deemed unnecessary because observations were only used following snowfall and after site clearing, therefore snow conditions at site *a*, which was never managed, were assumed to be always at their best, "fresh snow" conditions.

3.3 Characterization of sensors on-site

The theoretical method assumption is that, under the same conditions of snow cover, the difference of air temperature measurements between the two sensors at position *a* and position *b* (Δt_{site}) is zero. Undesired perturbations from nearby objects or topography should not be a factor for perfectly homogeneous sites. In real conditions such factors can hardly be neglected and a compromise is needed to minimize their influences from one side and have logistical opportunities (access, power, maintenance) on the other. To take this issue into account, the specific site conditions and environmental factors have been evaluated and a correction adopted. Non-symmetries can occur, for instance, in cases of variable wind direction and speed, asymmetric shadows or other non-homogeneous atmospheric or surface conditions, causing a non-null temperature difference between sensors in a pair.

A specific measurement campaign was therefore performed on site, after each snow event, before the snow removal from point *b*, to evaluate such possible systematic temperature differences Δt_{site} and their repeatability among the pairs of instruments. The following considerations were taken into account:

- data was recorded when snow was present below both the measurements points;
- data was selected during day time with incident solar radiation greater than zero;
- data was selected when the reflected radiation difference was zero (identical readings of the two radiometers facing the soil).

The readings of sensors pairs under these conditions have been recorded, systematic values Δt_{site} have been evaluated and used to correct the raw data recorded on site, with an associated uncertainty $u_{\Delta t_{site}}$. This uncertainty was evaluated as repeatability of the differences, and was deemed constant during the measurement campaign (November to March), because no significant changes in the nearby water flows (small rivers) was found and the pine trees vegetation remained constant. Events of asymmetric shadows, cast only over one of the two measurement points, due to a mountain peak occasionally projecting its shadow during the period of shortest daytime (December to January) were also identified: records associated to this shadowing effect were neglected form the data analysis, thus also from the evaluation of $u_{\Delta t_{site}}$. No mutual shadowing among instruments was observed, since the sun elevation and position over the surrounding mountain skyline was enough to avoid this phenomenon. Results of this characterization are presented in Table 4.

3.4 Uncertainty budget

The overall uncertainty budget $u_{\Delta t_{air}}$ for the temperature differences Δt_{air} has been derived according to the Guide to the expression of Uncertainty in Measurement (GUM) (JCGM, 2008), from the instruments characteristics and experimental conditions. As reported above, no calibration uncertainty components are here introduced, since the measurand is a relative difference, which does not require absolute accuracy.

The expression for the evaluation of overall uncertainty is defined as:

$$u_{\Delta t_{air}} = \sqrt{u_{res}^2 + u_{lab}^2 + u_{\Delta t_{instr}}^2 + u_{\Delta t_{site}}^2} \quad (2)$$

where:

- u_{res} is due to the resolution of instruments and data loggers as provided by manufacturers;
- u_{lab} is the component of uncertainty due to laboratory conditions and is composed by temperature uniformity and stability of the laboratory itself;
- $u_{\Delta t_{instr}}$ was evaluated during the laboratory testing of thermometers and is mainly ascribed to sensors short-term stability and statistical contributions;
- $u_{\Delta t_{site}}$ is related to the non-ideal characteristic of the site conditions.

As used in metrology, uncertainty is described in terms of coverage factor (a number larger than one by which a combined standard measurement uncertainty is multiplied to obtain an expanded measurement uncertainty, BIPM and Joint Committee For Guides In Metrology, 2008). Table 5 summarizes the components of uncertainty with the expanded uncertainty $U_{\Delta t_{air}}$ reported with coverage factor $k = 2$, meaning a confidence level of 95 %.

4. Data analysis and results

4.1 Data selection and method

The measurement campaign was performed between 8 September 2016 and 24 March 2017.

The sampling frequency of each pair of sensor was different but, in order to retain comparability, recording frequency was set to 10 min for all of them. During the campaign, an operator constantly accessed the experimental site and marked the best days for the analysis, in terms of sunny days (maximum radiation conditions) after a snowfall (highest albedo) when the snow below instruments at point *b* was recently removed (maximum expected differences).

Snow was removed on 4 days: 30 November, 22 December 2016, 20 January and 23 February 2017. Each time, snow was completely removed within the radius of 5 m, leaving the natural soil exposed. Salt was used each time to prevent the formation of ice, which would have changed the natural soil reflectivity, and to make snow removal easier and more complete. The data analysis was limited to measurements recorded in the days immediately after snow removal from point *b*.

Results showed that the albedo effect leads to larger Δt_{air} values during the central hours of days with high values of solar radiation and no wind. The effect was negligible or hidden under the general thermal noise and uncertainties in days characterised by fog, clouds cover or wind. In favourable weather conditions, daily measurements present a similar trend as the one showed in the example in Fig. 7, with night-time differences close to zero and a noise coherent with the instrumental relative uncertainty. In daytime, the effect emerges differently among the different systems.

Figure 8 shows the evolution of albedo with time, for the whole duration of the experiment, in both sites *a* and *b*. Differences are apparent, especially right after the four snow removals (marked as vertical dashed lines). The presence of outliers that fall above the theoretical albedo $\alpha = 1$ line can be explained in two ways: most of them happen when radiation values are low and uncertainties in their measurement are the larger (black dots). Others, at higher values of radiation (light dots), are due to snow covering the incident radiation detector: in fact, these values happen before a snow-clearing event (marked as vertical dashed lines) and are absent in the following days. The plot also shows indirectly the times of first snow and its complete natural thawing.

Differences of incident radiation in the two measurement points have also been evaluated and taken into account, in order to exclude the cases when these differences were significant and due for example to asymmetric shadows from clouds or occurrences of the mountain peak shadow as mentioned in Sect. 3.3. Having already excluded those values, measurements of

incident radiation were mostly consistent within instrumental uncertainty, which was evaluated to be 35 W m^{-2} on the basis of sensors characteristics such as sensitivity, repeatability and resolution. Records of temperature differences have been included in the data analysis only when the associated radiation difference was within this uncertainty value. As expected, due to the vicinity of the two measurement points, only few records were excluded due to larger incident radiation differences. On the other hand, reflected radiation in the two measurement points show very large differences due to the difference in reflectivity between snow-covered area and the snow-cleared area on point *a* (Fig. 9).

A threshold on the difference of reflected radiations, $\Delta Rad_{\mathrm{ref}} = 200\ \mathrm{W\ m^{-2}}$, was chosen in the selection of records with significant temperature differences, in order to better identify the largest values of the investigated effect. The threshold was chosen by observing that, below that value, the distribution of temperature differences between the two measuring points matched the overall measurement uncertainty. An attempt to include data also below this threshold cut limit was conducted, resulting in a large amount of data with temperature differences below 0.1 °C, thus extending the 0 – 0.2 °C range (first bar of graph in Fig. 10). The resulting plot would decrease its graphical information in the highest and most important difference values, which result "compressed" thus less detailed. Moreover, below such threshold it was impossible to discriminate among the different kind of sensors and shields.

In Fig. 9, plots (a) and (b) show the reflected radiation recorded in position *a* and *b* during the entire period. Plot (c) shows the differences of the reflected radiation recorded with and without snow with threshold value (straight horizontal line).

On this subset, a further data selection is applied, by excluding the values of temperature differences among pairs of sensors that fall below the Δt_{site}. This is the reason why the total number of significant records are not the same for all pairs of instruments. The number of available data for each pair was found to be proportional to the amplitude of the albedo effect. This result is not surprising, since when the differences distribution is skewed towards larger values, it follows that more temperature differences are found above the Δt_{site} limit. This is clearly evidenced in Fig. 11.

4.2 Results

As a preliminary analysis, records from the deployed instruments were initially considered as a single set. The plot in Fig. 10 shows the distribution of Δt_{air} grouped in bins of 0.2 °C regardless of the sensor typologies.

The most frequent values of Δt_{air} are found between 0 °C and 0.4 °C, with a significant number of records between 0.4 °C and 1.6 °C. The least populated classes are from 2 °C to 4 °C. Maximum Δt_{air} values ranged up to 3.8 °C while 95 % of the values were found to be within 2.4 °C, which can be considered the highest significant value for this specific experiment.

Records where then segregated according to system types as reported in the following plots (Fig. 11). The analysis shows that no instrument is immune from the effect, resulting in different values of Δt_{air} depending on the different technical features. As in the previous histogram (Fig. 10), most records are concentrated between 0 °C and 2 °C. Looking at each pair of instruments (intended as sensor+shield configuration), it is clear that Types B and F show the widest ranges of Δt_{air}, reaching up to respectively 3.1 °C and 3.8 °C. The temperature differences for Types A, C and D were always under 1.5 °C, while Type E reaches 2 °C; almost all records of these four Types, though, were concentrated between 0 °C and 1 °C.

Given that we had only one type of actively ventilated shield, and many passively ventilated shields with different designs, it does not seem fair to draw general conclusions about actively vs. passively ventilated shields. It is interesting to note, however, that actively ventilated shields are not necessarily the best performers; for instance, Type D system performance with a passive screen is similar to that of type A system. It must be kept in mind, though, that A and D systems feature different screens but also different sensors (Pt100 vs thermo-hygrometer), so a straightforward comparison is difficult. Helical shields may perform better with respect to other multi-plate shields, possibly because they maximize air intake effectively cooling down the sensor inside; this is something, however, to be investigated perhaps with a theoretical study.

Table 6 summarises the maximum Δt_{air} for each instrument type, with the associated uncertainty.

4.2.1 Wind speed and radiation effects

Further data analysis was addressed to evidence the relations between temperature differences and the main quantities of influence, such as wind speed and radiation.

Fig. 12 shows Δt_{air} values, as calculated in previous Section, as a function of wind speed. Values between 0 and 5 m s^{-1} were observed; as expected, stronger winds significantly reduce the albedo effect due to air mixing in the sensor area and to the increase in heat dissipation by convection. For speeds greater than 3 m s^{-1} the effect was clearly reduced in all systems. In other similar experiments about obstacle effects on near-surface temperature measurements, it often emerges the fact that wind dominates radiation: for instance Coppa et al., (2021b) showed that, in case of strong winds, turbulent mixing of heat to higher atmospheric layers makes its influence on temperature lower at 2 m where the sensors are located.

In the same plot, measurements are coded in cyan scale to underline the difference of reflected radiation, $\Delta Rad_{\mathrm{ref}}$, associated to each Δt_{air}. In general, large $\Delta Rad_{\mathrm{ref}}$ are associated to large Δt_{air}, especially associated to winds between 1 and 2 m s^{-2}: this may be due to a selection bias, given that stronger winds are more frequent in the central hours of the day, when incident radiation (and therefore $\Delta Rad_{\mathrm{ref}}$) is higher. To better evidence the behaviour of albedo effect, Fig. 13 shows values of Δt_{air} as a function of $\Delta Rad_{\mathrm{ref}}$. In the plots, a positive trend of Δt_{air} is apparent for type B and type F instruments, but the large scatter masks the relation.

5. Discussion

The analysis here presented shows that the reflected radiation from a snow-covered surface affects the reliability of meteorological thermometers by transferring extra heat. This effect results in a temperature increase, here evaluated between identical co-located sensors, over snow-free ground.

The main considerations are here summarised:

- Some typologies of instruments are more influenced than others, with significant differences (over 3 °C);
- Out of the whole group of instruments, 95 % of temperature differences were found within 2.4 °C;

- The lowest temperature mean differences have been recorded by forced ventilated shields; among the naturally ventilated shields, by those with helical shapes;
- Most highest temperature differences were found in conjunction with the maximum reflected radiation differences between the two positions, as expected;
- The wind has the effect of reducing the highest temperature differences;
- The overall uncertainty on temperature differences in field conditions ranged between 0.1 °C and 0.4 °C in $k = 2$;
- The distribution of differences as a function of the reflected radiation was found, for most instruments, to be uniform; some instruments show a large scatter in this relation.

Although limited in number, the instruments selected covered most commercial configurations of modern meteorological sensors with a reasonable balance of fan aspirated, naturally ventilated and alternative designs. While the duration of the experiment was limited by the duration of the funded project that backed it, almost all meteorological conditions in the site were met, including radiation and wind variability, during the November-to-March time span. Moreover, an appropriate site with easy access for maintenance, long-lasting presence of snow, electric current, staff presence is not an easy find, especially in Alpine valleys. Considerations on possible effects of the site features (trees, small building, shadow) were in any case made, to select data and correct for systematic effects.

For these reasons, these results are considered valid to understand the order of magnitude of the effect. This work also gives an example on how to evaluate this phenomenon and take it into account in terms of correction and associated uncertainty. Following these guidelines, manufacturer and end users are encouraged to characterise their own instruments to evaluate the albedo effect as a function of reflected radiation, wind speed etc, to obtain a correction function. Since there is no certainty that a complete correction function can be calculated, also in the case of a single instrument, the level of approximation that can be achieved must be taken into account.

Very few are the examples in scientific literature of similar evaluations, methods or prescriptions to quantify the studied effect on near-surface thermometers. The work by Huwald et al., (2009), mentioned in the introduction, where one meteorological station (featuring, among other ancillary sensors, albedometers, platinum thermometers and several three-dimensional sonic anemometers used as temperature references) was installed on a Swiss glacier, reaches the same conclusions that "Temperature errors decrease with decreasing solar radiation and increasing wind speed" and that this effect ranges in the order of degrees Celsius. With respect to the aforementioned study, the key improvement of the work here presented was the use of different sets of identical instruments; the effect is evaluated in a relative way, without the assumption that a sonic anemometer can be used as unbiased reference. It is agreed that non-contact thermometry is immune from some effects of the influencing quantities, but the accuracy achieved by using anemometers as thermometers is not sufficient for being considered a reference instrument (Burns et al., 2012; Richiardone et al., 2012). The method here proposed can be adopted just by using a second identical thermometer and shield, significantly reducing costs. The resulting uncertainties are reduced with respect to comparing different systems and even different physical principles in measuring air temperature. Finally, in this analysis the

investigation was extended to more different kinds of sensors and shields, thus making the results representative of a wider typology of solutions adopted in meteorology.

It must be noted that, since no reference air temperature independent from radiation errors is available, the total uncertainty due to heating of the sensor by solar radiation cannot be accurately and absolutely quantified. As a matter of fact, albedo-induced uncertainty does not include radiative errors due to heating of the sensor shield from incident solar radiation; this should be added to determine a complete shortwave radiation-induced uncertainty on air temperature measurements. In any case, this would go beyond the scope of the work, given that it focused on relative differences caused by reflected radiation only, and that there is much more literature dealing with the effect of incident radiation. Erell et al., (2005), for instance, showed that no shield provides complete protection from incident radiation, with relative uncertainties up to 1.5 °C; Lopardo et al., (2014), showed that an aged, darkened screen can introduce uncertainties up to a similar values, especially at daily maxima.

Beside delivering the numerical results, the key output of this work is a methodology for evaluating a factor affecting temperature data in climatology (and meteorology) and give an example on how this can be implemented and adopted when selecting instruments and shields as in the case of surface stations of climatological networks.

6. Recommendations to users and manufacturers

The main purpose of the paper is to quantify the albedo effect involving different configurations to obtain a result as general as possible. However, the analysis is still limited to some possible configurations and the aim of the work is not to influence or direct the choice of a configuration. For this reason, no recommendation on "which system to buy" will be given in this paper, because no general rule can be drawn: the fan-aspirated system performed generally well, but it was outperformed by some of the passive screens, especially at winds around 2 m s^{-1}; size does not seem crucial (systems C and D), while shape does (systems E and F); on the other hand, similar shapes can give very different results (systems B and C).

One of the main tasks of the MeteoMet project was to give metrological support to the meteo-climatology community, including data users, station staff and manufacturers (Merlone et al., 2018). A summary of the outcomes of this work has been presented at the WMO CIMO TECO 2018 (Musacchio et al., 2018) and sent to the WMO CIMO expert team on Observation In-Situ technologies (now Expert team on Surface and sub-surface measurements and Expert team on Measurement Uncertainties of the Infrastructure Commission).

Following the publication of the experimental method (Musacchio et al., 2019) indications on how to design and implement a field experiment, to evaluate the errors in temperature readings in thermometers positioned above snow-covered land have been prepared and sent to WMO expert teams on "Metrology", "Surface Measurements" and "Measurement Uncertainties". Manufacturers should also evaluate and declare this effect on their product datasheets and where possible adopt solutions to minimize it.

The indication to WMO is summarised as follows.

To evaluate the amplitude of the error due to reflected radiation from snow covered soil on specific instruments, it is recommended that a specific analysis is performed, following the procedure here reported:

a) *Two identical systems (thermometers and shield, possibly using the same data logger) must be installed in proximity (between 20 and 50 m of distance): one positioned above a snow-covered area and one above an area where snow is removed at any snow event.*
b) *Further instrumentation is required to constantly record and monitor the environmental factors of influence: direct and reflected radiation in both areas, wind speed and direction, humidity*.
c) *Readings should be recorded for at least one full snow season, to meet most meteorological conditions of the sites and evaluate the associated effects and factors of influence.*
d) *A correction can then be generated in terms of a relationship between temperature reading differences with respect to the reflected radiation, wind speed and air temperature.*
e) *The uncertainty budget associated to the correction is then evaluated through Gaussian propagation: components of uncertainty are calculated by field analysis of systematic differences in temperature and by knowledge of each involved instrument performance, including radiometers and anemometers, and from the statistical analysis and interpolation.*

The objective of the recommendation is to report and inform users and instrument manufacturers to consider, include in data products and possibly minimize the effect of reflected radiation from a snow-covered surface on their systems. While the present study involved different typologies of solar shields, as an overall analysis with a significant variety of system available in the market, the recommendation is addressed to users and manufacturers for a direct evaluation on their specific system. More detailed analysis can then be adopted and a correction curve, with associated uncertainty, can be obtained and applied to post-processed data. This correction can compensate only the relative differences, with and without snow, not the overall radiation-induced biases.

The procedure and error evaluation process is also relevant for the definition of data quality and instrument features by the GCOS and the WMO in promoting climatological reference stations and the GCOS Surface Reference Network (GSRN). For high quality installations and climate reference stations, the analysis here presented can lead to data quality improvement by adding an evaluated relative correction and associated uncertainty.

7. Conclusions

The study here presented was performed to evaluate the accuracy of near-surface air temperature data series, recorded by thermometers in radiation shields positioned above snow. The study strictly followed an already published method and its associated experimental protocol. It involved a representative number of modern sensors and solar shields, including naturally ventilated, fan-aspirated and helical shields, provided as commercially offered by manufacturers, equipped with dedicated data loggers. The effect was apparent for all the systems, with maximum Δt_{air} values observed in absence of wind and at high

reflected radiation conditions such as in sunny days with clean fresh snow. The maximum Δt_{air} ranged from 1.2 °C to 3.8 °C, with the latter value achieved by sensor F, in conditions of low winds (~1 m s^{-1}), large difference between reflected and incident radiation (~ 350 W m^{-2}) and high incident radiation (>500 W m^{-2}).

The method was validated by the experimental results and can be considered a procedure for further similar investigations involving other typologies of sensors. This process can be adopted by manufacturers to test and characterise their product as well as by station staff and data users to include this effect, correction and associated uncertainty to the records. A similar analysis should be performed when selecting instruments to take part in a climate reference network, such as the planned GCOS Surface Reference Network GSRN, for those stations positioned on sites with snow presence.

Finally, further work can be addressed to the evaluation of correction curves in the form of temperature difference relationship with reflected radiation and wind conditions. The calculation of a correction function requires longer time of field activities, to meet the wider range of atmospheric conditions as well as have more data available for statistical analysis. The uncertainty budget associated to the curve will then be completed by including the statistical analysis and all components from the instruments involved: thermometers, anemometers and radiometers.

In a site where a high-quality installation is planned to be permanent, a study like this is recommended among the overall efforts to increase data quality and understand uncertainties in meteorological observations for climate.

Data availability

Original raw data is available at Zenodo.org (Coppa et al., 2021a)

Author contributions

Chiara Musacchio, Graziano Coppa and Andrea Merlone designed and run the experiment, with contributions by all co-authors. Laura Massano performed the data analysis with contributions by CM and GC. CM prepared the manuscript with contributions from all co-authors. Revisions were handled by GC, with contributions by CM and AM.

Acknowledgments

The authors wish to thank the Agenzia Regionale per la Protezione Ambientale del Piemonte, the Municipality of Balme and the “Les Montagnards” mountain hut for the valuable support, as well as the manufacturers that took part in the experiment by providing the instrumentation.

This work is being developed within the frame of the EMRP (European Metrology Research Programme) joint research project “MeteoMet 2”. The EMRP is jointly funded by the EMRP participating countries within EURAMET and the European Union.

References

Barry, R. and Blanken, P.: Microclimate and Local Climate, Cambridge University Press, Cambridge., 2016.

BIPM: Le Système International d'unités. [online] Available from: https://www.bipm.org/documents/20126/41483022/SI-Brochure-9.pdf/fcf090b2-04e6-88cc-1149-c3e029ad8232, 2019.

BIPM and Joint Committee For Guides In Metrology: Evaluation of measurement data — Guide to the expression of uncertainty in measurement. [online] Available from: http://www.bipm.org/en/publications/guides/gum.html, 2008.

Bohren, C. F. and Beschta, R. L.: Snowpack albedo and snow density, Cold Reg. Sci. Technol., 1(1), 47–50, doi:10.1016/0165-232X(79)90018-1, 1979.

Burns, S. P., Horst, T. W., Jacobsen, L., Blanken, P. D. and Monson, R. K.: Using sonic anemometer temperature to measure sensible heat flux in strong winds, Atmos. Meas. Tech., 5(9), 2095–2111, doi:10.5194/amt-5-2095-2012, 2012.

Burt, S. and de Podesta, M.: Response times of meteorological air temperature sensors, Q. J. R. Meteorol. Soc., 146(731), 2789–2800, doi:10.1002/qj.3817, 2020.

Camuffo, D. and Jones, P.: Improved Understanding of Past Climatic Variability from Early Daily European Instrumental Sources, edited by D. Camuffo and P. Jones, Springer Netherlands, Dordrecht., 2002.

CCT: Strategy Document for Rolling Programme Development for 2018 to 2027. The Consultative Committee for Thermometry., 2017.

Coppa, G., Musacchio, C. and Merlone, A.: Albedo effect experiment, , doi:10.5281/zenodo.5126973, 2021a.

Coppa, G., Quarello, A., Steeneveld, G., Jandrić, N. and Merlone, A.: Metrological evaluation of the effect of the presence of a road on near-surface air temperatures, Int. J. Climatol., 41(6), 3705–3724, doi:10.1002/joc.7044, 2021b.

Erell, E., Leal, V. and Maldonado, E.: Measurement of air temperature in the presence of a large radiant flux: An assessment of passively ventilated thermometer screens, Boundary-Layer Meteorol., 114(1), 205–231, doi:10.1007/s10546-004-8946-8, 2005.

GCOS: GCOS Surface Reference Network (GSRN): Justification, requirements, siting and instrumentation options. [online] Available from: https://library.wmo.int/doc_num.php?explnum_id=6261, 2019.

Huwald, H., Higgins, C. W., Boldi, M. O., Bou-Zeid, E., Lehning, M. and Parlange, M. B.: Albedo effect on radiative errors in air temperature measurements, Water Resour. Res., 45(8), 1–13, doi:10.1029/2008WR007600, 2009.

Lacombe, M., Bousri, D., Leroy, M. and Mezred, M.: Instruments and Observing Methods report No . 106 WMO Field Intercomparison of Thermometer Screens/Shields and Humidity Measuring Instruments., 2011.

Lopardo, G., Bertiglia, F., Curci, S., Roggero, G. and Merlone, A.: Comparative analysis of the influence of solar radiation screen ageing on temperature measurements by means of weather stations, Int. J. Climatol., 34(4), 1297–1310, doi:10.1002/joc.3765, 2014.

Merlone, A., Lopardo, G., Sanna, F., Bell, S., Benyon, R., Bergerud, R. A. A., Bertiglia, F., Bojkovski, J., Böse, N., Brunet, M., Cappella, A., Coppa, G., del Campo, D., Dobre, M., Drnovsek, J., Ebert, V., Emardson, R., Fernicola, V., Flakiewicz, K.,

Gardiner, T., Garcia-Izquierdo, C., Georgin, E., Gilabert, A., Grykalowska, A., Grudniewicz, E., Heinonen, M., Holmsten, M., Hudoklin, D., Johansson, J., Kajastie, H., Kaykisizli, H., Klason, P., Kňazovická, L., Lakka, A., Kowal, A., Müller, H., Musacchio, C., Nwaboh, J., Pavlasek, P., Piccato, A., Pitre, L., de Podesta, M., Rasmussen, M. K., Sairanen, H., Smorgon, D., Sparasci, F., Strnad, R., Szmyrka- Grzebyk, A. and Underwood, R.: The MeteoMet project - metrology for meteorology: Challenges and results, Meteorol. Appl., 22(January), 820–829, doi:10.1002/met.1528, 2015a.

Merlone, A., Musacchio, C. and Sanna, F.: The Metrology for Meteorology Conference: MMC 2014, Meteorol. Appl., 22, 817–819, doi:10.1002/met.1548, 2015b.

Merlone, A., Sanna, F., Beges, G., Bell, S., Beltramino, G., Bojkovski, J., Brunet, M., del Campo, D., Castrillo, A., Chiodo, N., Uytun, A., Voldan, M., Colli, M., Coppa, G., Cuccaro, R., Dobre, M., Drnovsek, J., Ebert, V., Fernicola, V., Garcia-Benadí, A., Garcia-Izquierdo, C., Gardiner, T., Georgin, E., Gonzalez, A., Groselj, D., Heinonen, M., Hernandez, S., Högström, R., Hudoklin, D., Kalemci, M., Kowal, A., Lanza, L., Miao, P., Musacchio, C., Nielsen, J., Nogueras-Cervera, M., Oguz Aytekin, S., Pavlasek, P., de Podesta, M., Rasmussen, M. K., Del-Río-Fernández, J., Rosso, L., Sairanen, H., Salminen, J., Sestan, D., Šindelářová, L., Smorgon, D., Sparasci, F., Strnad, R., Underwood, R., Uytun, A. and Voldan, M.: The MeteoMet2 project—highlights and results, Meas. Sci. Technol., 29(2), 025802, doi:10.1088/1361-6501/aa99fc, 2018.

Musacchio, C., Massano, L., Coppa, G., Merlone, A. and Hofstaetter, C.: Effect of snow-reflected radiation in near surface air temperature, in The 2018 WMO/CIMO Technical Conference on Meteorological and Environmental Instruments and Methods of Observation (CIMO TECO-2018)2., 2018.

Musacchio, C., Coppa, G. and Merlone, A.: An experimental method for evaluation of the snow albedo effect on near-surface air temperature measurements, Meteorol. Appl., 26(1), 161–170, doi:10.1002/met.1756, 2019.

Nigrelli, G., Fratianni, S., Zampollo, A., Turconi, L. and Chiarle, M.: The altitudinal temperature lapse rates applied to high elevation rockfalls studies in the Western European Alps, Theor. Appl. Climatol., 131(3–4), 1479–1491, doi:10.1007/s00704-017-2066-0, 2018.

Richiardone, R., Manfrin, M., Ferrarese, S., Francone, C., Fernicola, V., Gavioso, R. M. and Mortarini, L.: Influence of the Sonic Anemometer Temperature Calibration on Turbulent Heat-Flux Measurements, Boundary-Layer Meteorol., 142(3), 425–442, doi:10.1007/s10546-011-9688-z, 2012.

Stevenson, T. C. E.: New description of box for holding thermometers, J. Scottish Meteorol. Soc., 1, 122, 1864.

Thorne, P. W., Diamond, H. J., Goodison, B., Harrigan, S., Hausfather, Z., Ingleby, N. B., Jones, P. D., Lawrimore, J. H., Lister, D. H., Merlone, A., Oakley, T., Palecki, M., Peterson, T. C., de Podesta, M., Tassone, C., Venema, V. and Willett, K. M.: Towards a global land surface climate fiducial reference measurements network, Int. J. Climatol., 38(6), 2760–2774, doi:10.1002/joc.5458, 2018.

WMO: WMO/CIMO #8 Guide to meteorological instruments and methods of observation. [online] Available from: https://library.wmo.int/index.php?id=12407&lvl=notice_display, 2012.

Xiong, C., Shi, J., Ji, D., Wang, T., Xu, Y. and Zhao, T.: A New Hybrid Snow Light Scattering Model Based on Geometric Optics Theory and Vector Radiative Transfer Theory, IEEE Trans. Geosci. Remote Sens., 53(9), 4862–4875,

565 doi:10.1109/TGRS.2015.2411592, 2015.

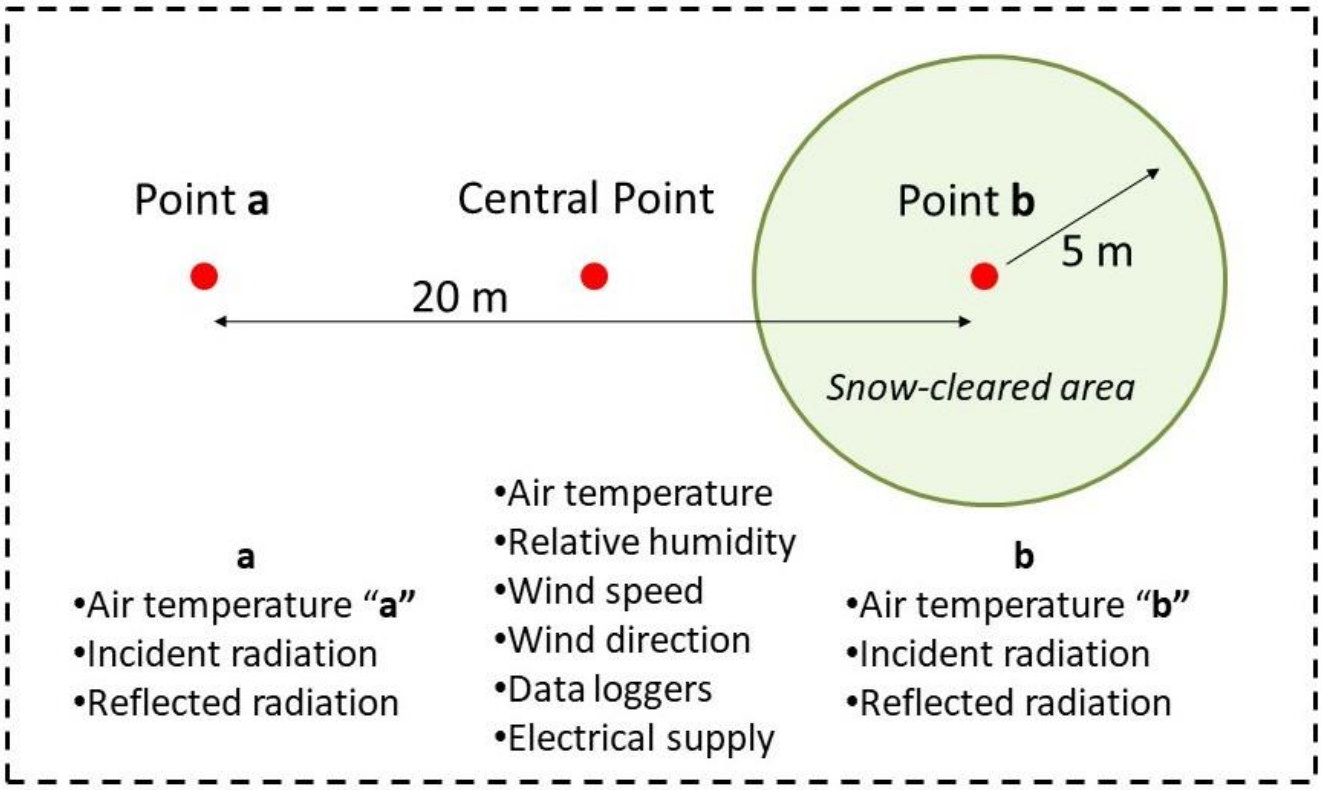

Figure 1: Scheme of the installation area. Points "*a*" and "*b*" host the pairs of identical thermometers and shields. The central point hosts auxiliary equipment, data loggers and sensors for measuring quantities of influence.

Figure 2: Some of the collected instrument pairs ready for the laboratory characterisation.

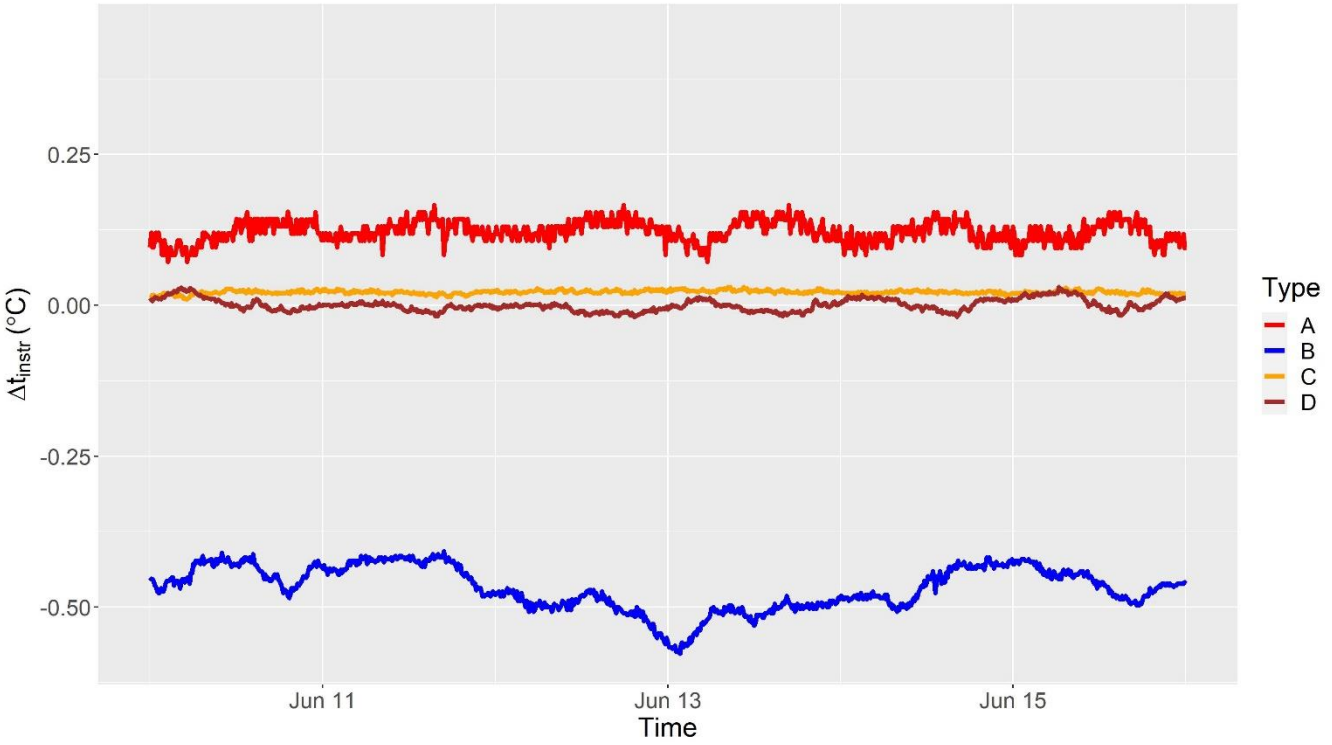

575 **Figure 3: Example of laboratory characterisation. One-week acquisition, at 10-min sampling rate, of differences between the readings of the two sensors of the pair. E and F sensors were not available at the time of laboratory characterisation. Negative and positive differences are only due to arbitrary conventions on labelling "first" and "second" sensors in a pair.**

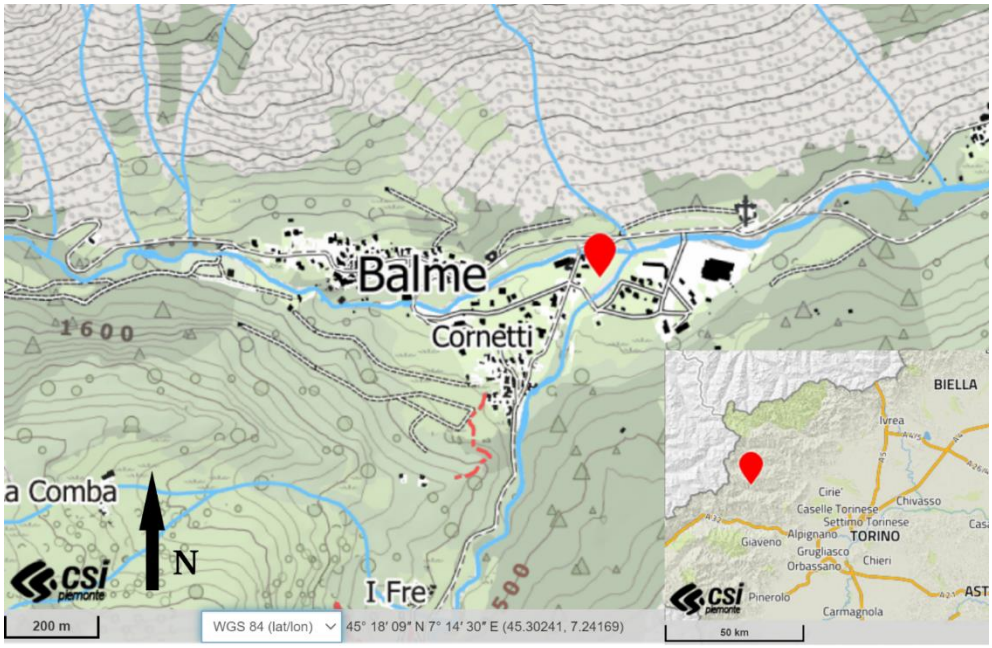

(a)

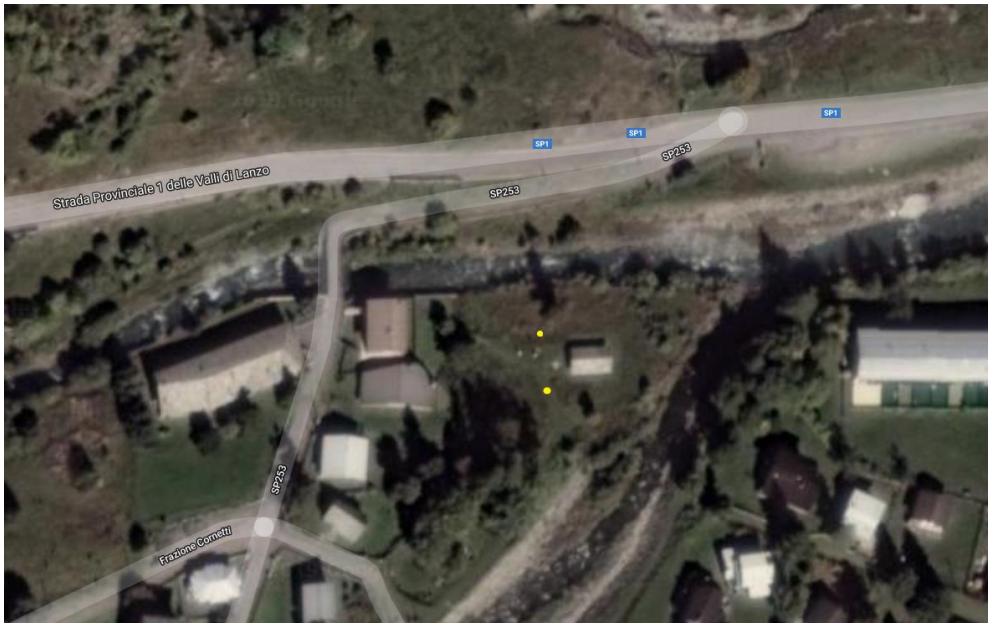

(b)

Figure 4: (a) Local topographic map (© Geoportale Regione Piemonte, 2021) of the area (~ 2x1.5 km) surrounding the measurement site. The Ala valley is aligned in an East-West way: mountains close the valley from the North, while on the South a small lateral valley opens up the horizon to other high mountains. The measurement site is marked with a red teardrop flag. The inset show the position of the measurement site in the Western Alps and with respect to Turin. (b) Zoomed in (~200x100 m) Google Earth (© Google 2017) picture of the experimental site. The approximate positions of the two measurement stations are marked by the yellow spots.

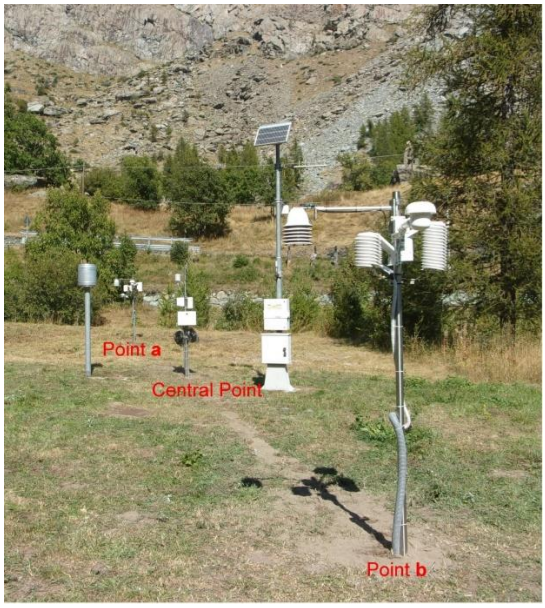

(a)

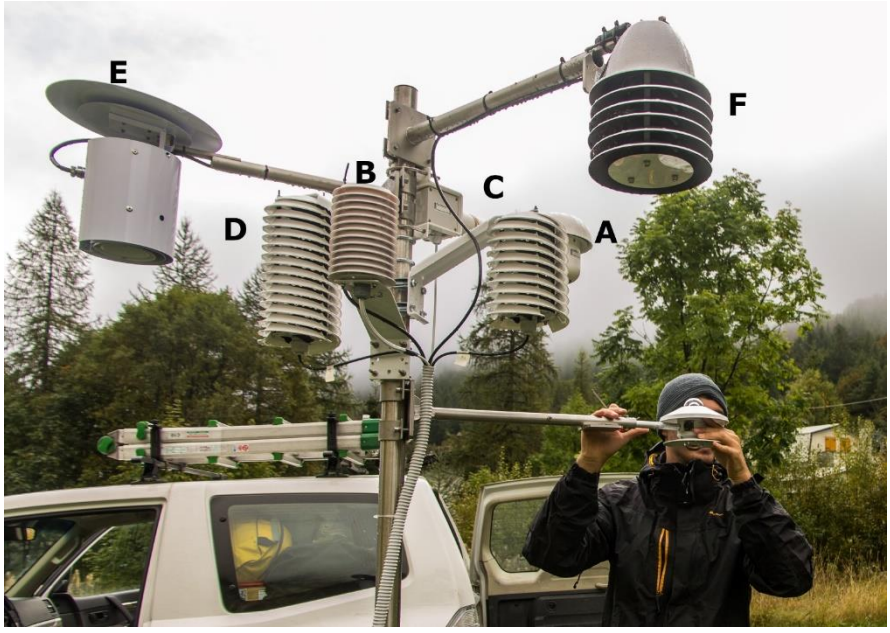

(b)

Figure 5: (a) The experimental site in summer, during the installation of the instruments. Radiometers and sensors E and F were not yet installed at the time of this picture. (b) Close-up of one experimental station, during final phase of installation, with all systems labelled as in Table 1.

(a)

(b)

Figure 6: (a) The measurement site in its snow-covered configuration. In the background position *a*, where snow will be left. In the foreground position *b*, with snow still to be removed. (b) Point *b* in snow-removed condition.

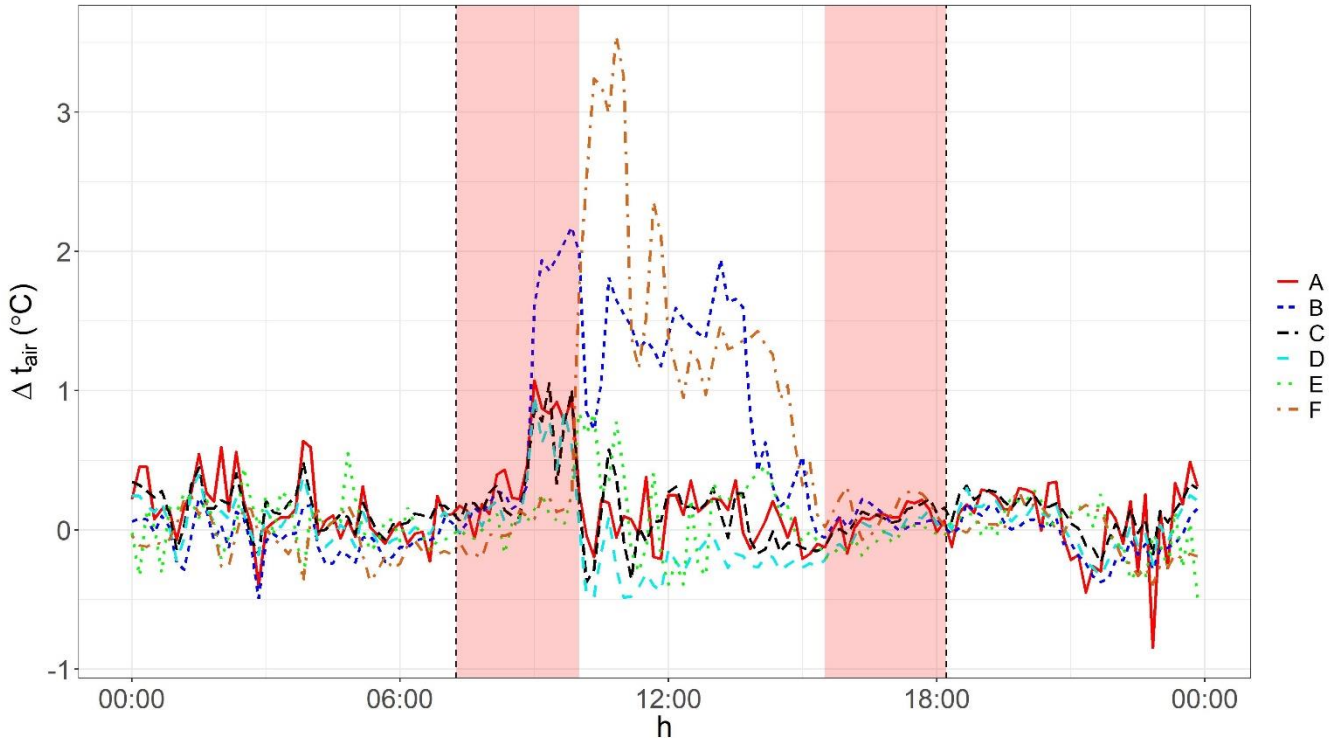

Figure 7: A typical plot of a one-day-long acquisition, demonstrating the effect in terms of temperature differences Δt_{air} (defined in the text as Equation 1) among pairs of identical sensors (25 February 2017). The day has been selected as a representative example, with snow removed a few days before. Weather was mainly sunny, with maximum incident radiation of 700 W m^{-2}, maximum reflected radiation of 500 W m^{-2} in snow condition and less than 100 W m^{-2} in the snow-free area. Vertical dashed lines represent sunset and sunrise times, while shaded areas mark the periods when incident radiation on the sensors was < 300 W m^{-2} (no or faint direct sunlight). Hours are reported in local time (Central European Time - CET).

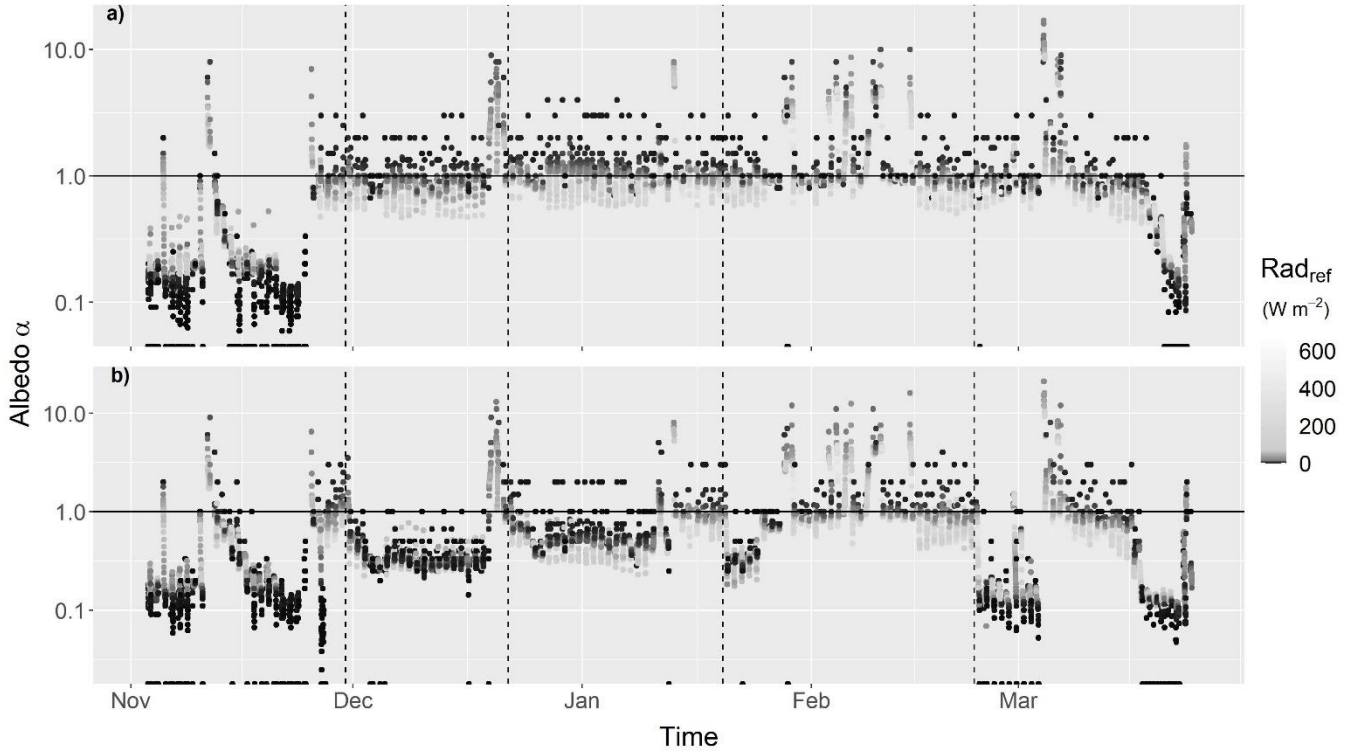

Figure 8: Plots of albedo (in logarithmic scale), calculated as ratio of reflected and incident radiation, for a) snow-covered and b) snow-cleared site. The horizontal black line represents the theoretical maximum value of albedo ($\alpha = 1$), while vertical dashed lines mark the snow removal events. Data points are coded in greyscale as a function of reflected radiation.

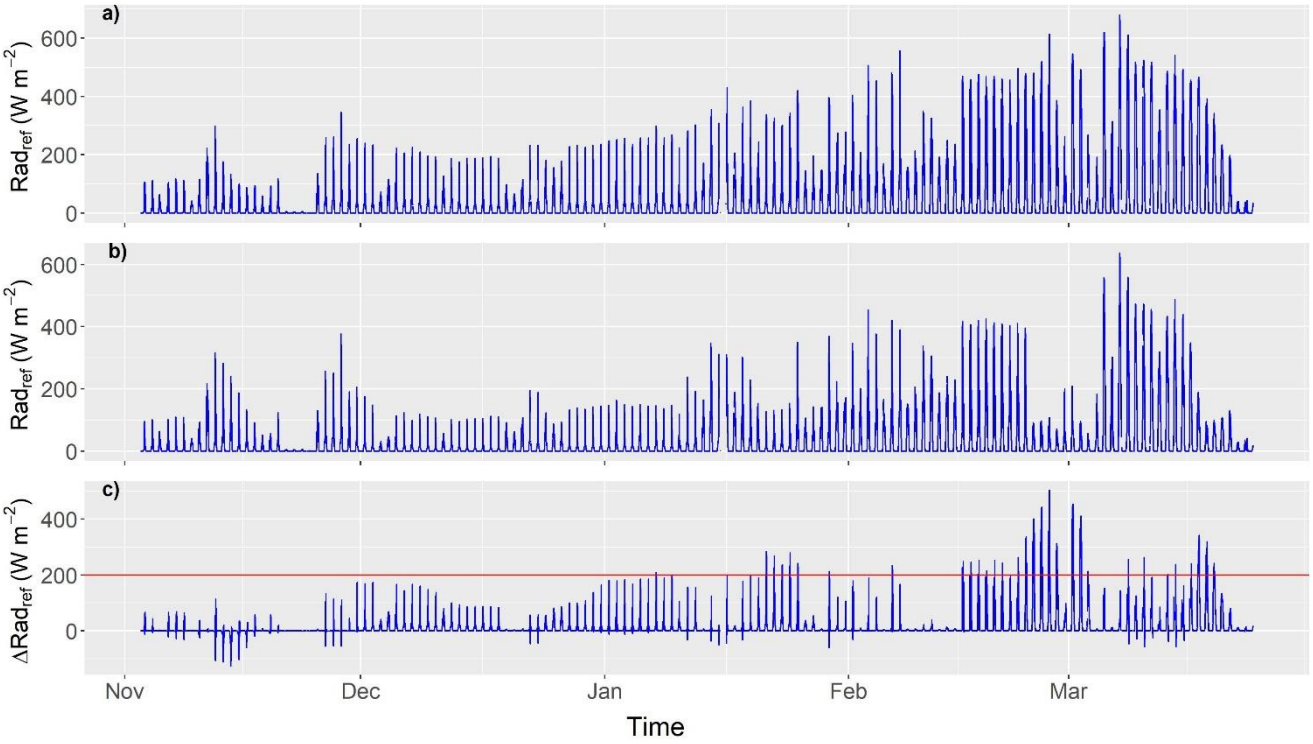

Figure 9: Results of measured reflected radiation (the whole 10-min sampled dataset) recorded in position *a* - sensor above snow (a), and *b* – sensor above snow-cleared area (b) during the entire period of the experiment. Differences of reflected radiation recorded in position *a* and *b*, ΔRad_{ref}, are shown in (c). The threshold (horizontal line in plot c) chosen to better discriminate the temperature differences from the overall uncertainty in temperature records is shown. Negative values in panel (c) are mostly due to errors in radiation measurements being larger than the measurement values themselves, like what isas shown in Figure 8. The cluster of negative values reaching -100 W m^{-2} around 14 November happened before the first snow event, so not due to snow.

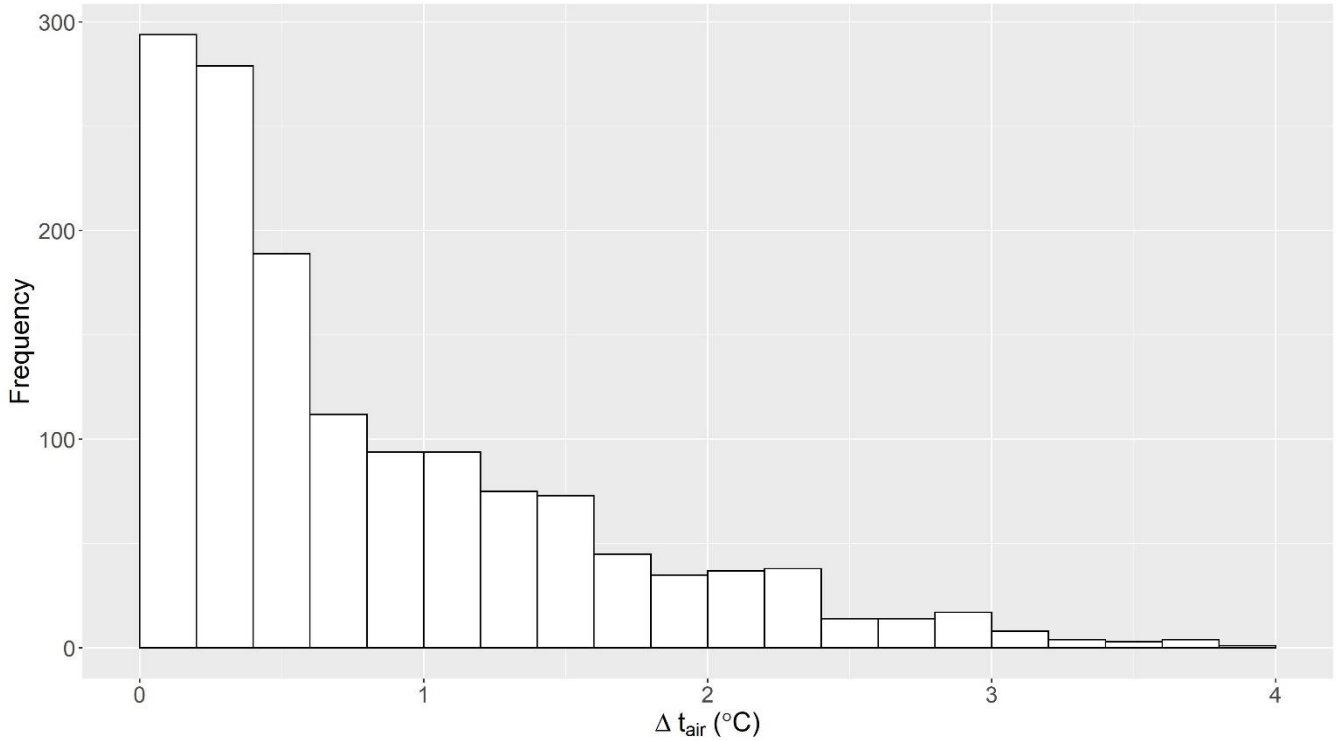

Figure 10: Frequency of temperature differences, Δt_{air}, considering all pairs of instruments, of records exceeding the selected threshold for reflected shortwave radiation of 200 W m^{-2}.

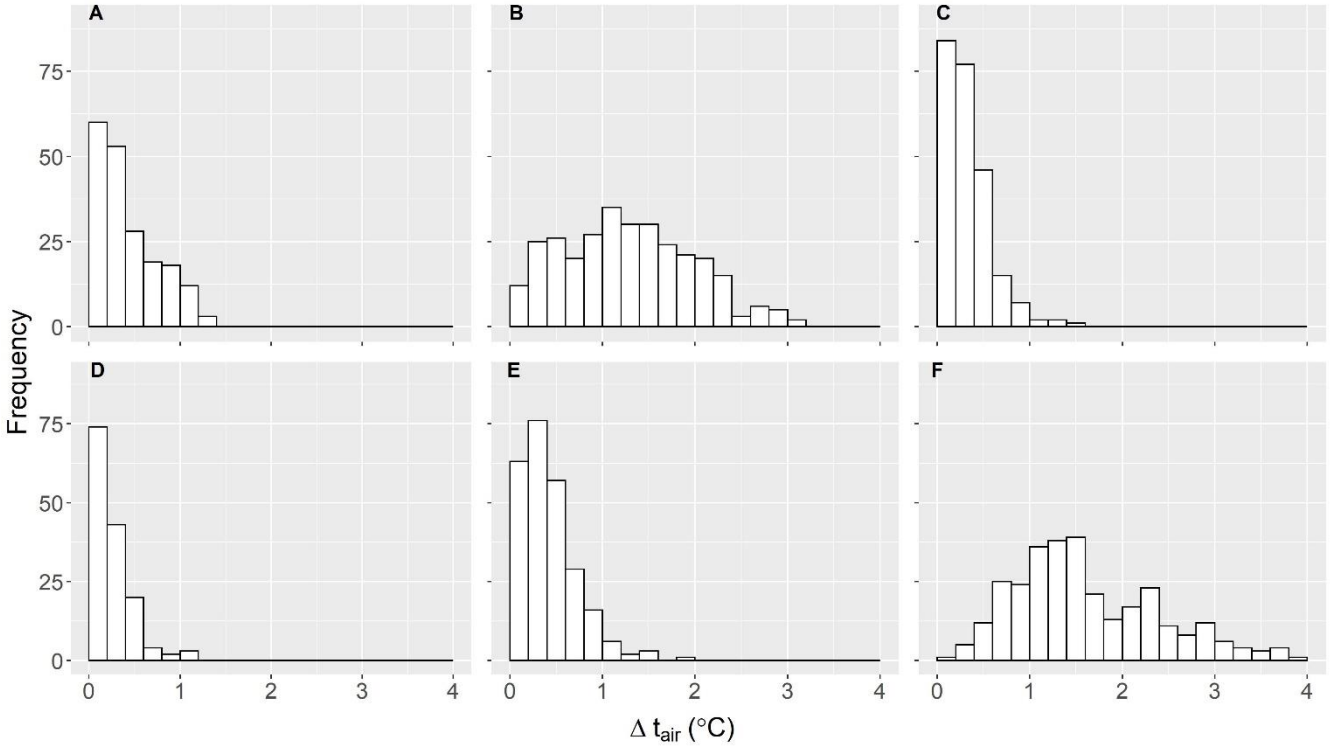

630

Figure 11: Results of evaluation of Δt_{air} for each pair of sensors. Instrument types are identified with letters from A to F (refer to Table 1 for identification). The histogram is divided in bins of 0.2 °C and the number of occurrences of Δt_{air} is shown for each instrument.

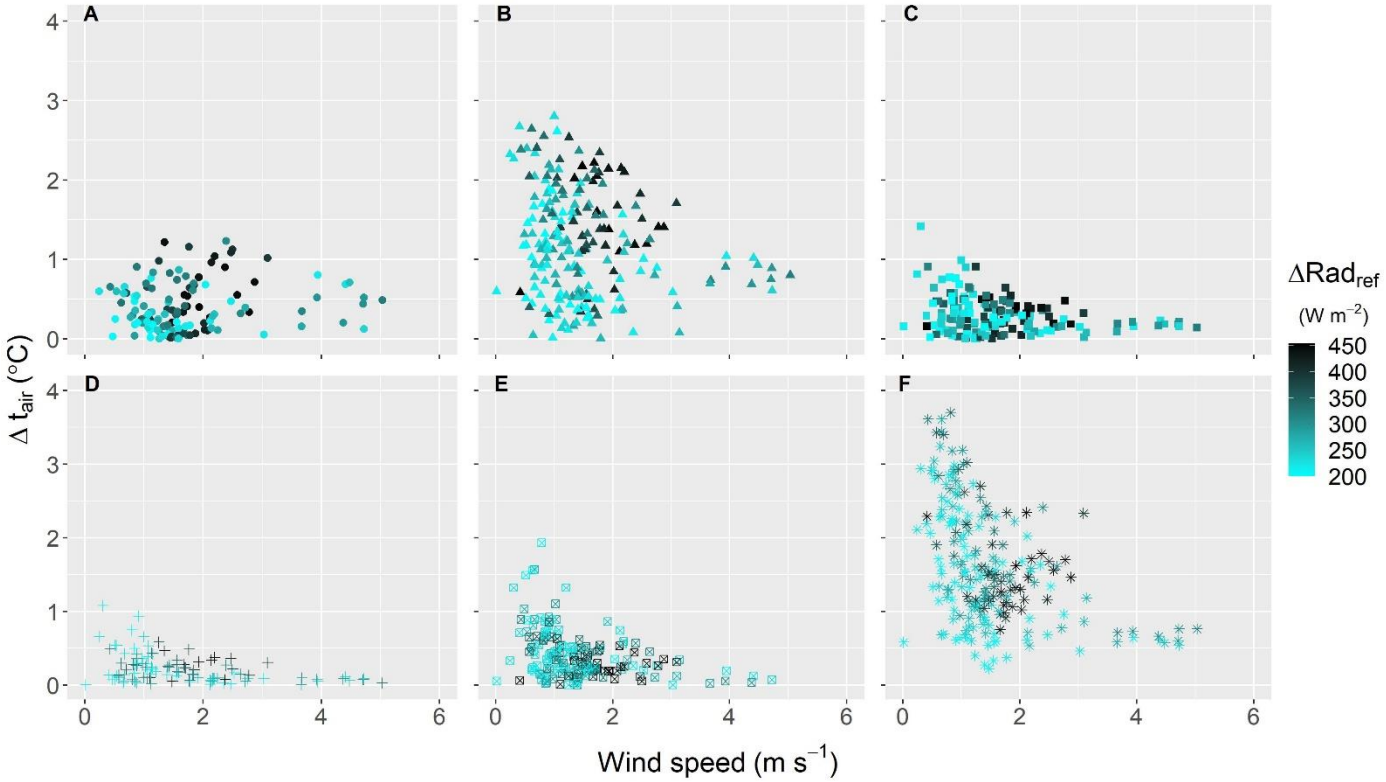

635

Figure 12: Temperature difference Δt_{air} measured as a function of wind speed for all the instrument type A-F. Cyan scale is used to evidence the value of the difference of reflected radiation, $\Delta Rad_{\mathrm{ref}}$,related to each value of Δt_{air} reported.

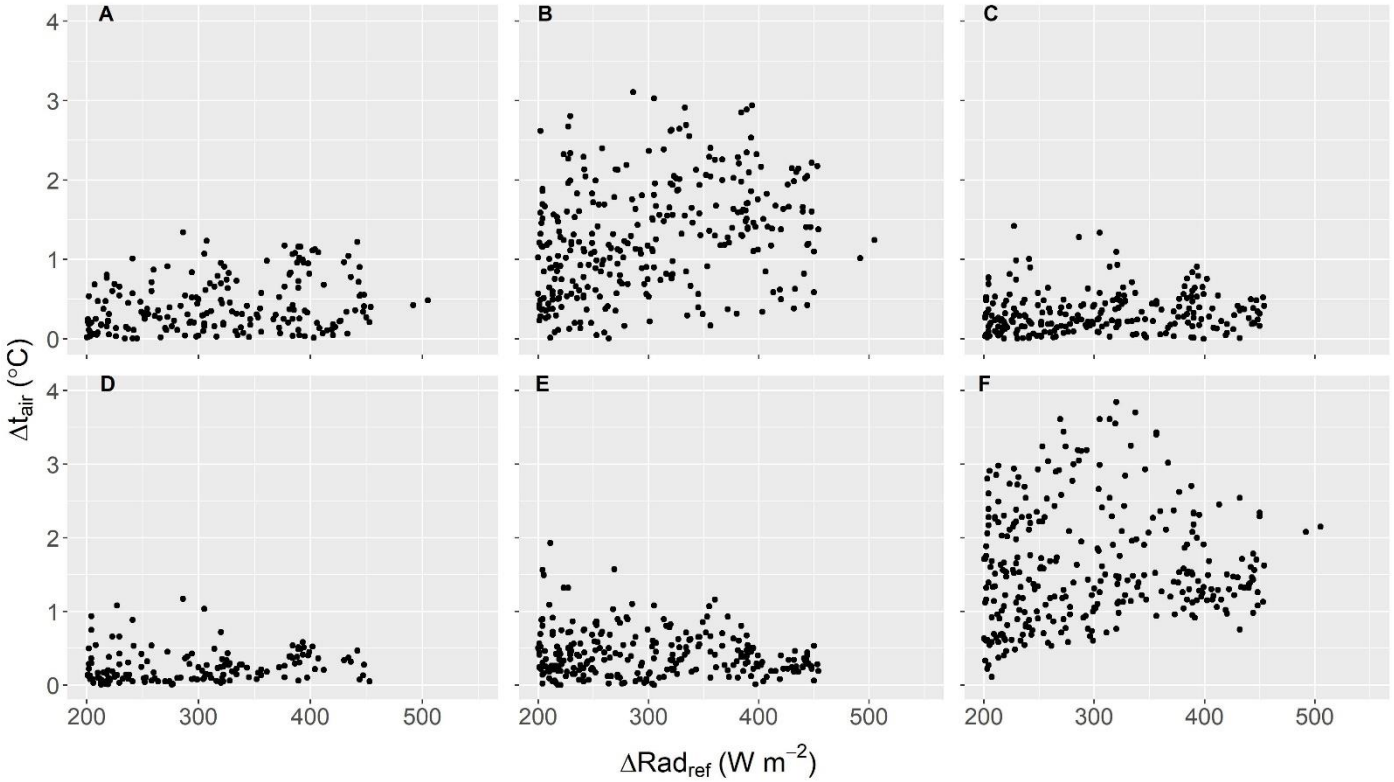

Figure 13: Temperature differences Δt_{air} evaluated in the data analysis plotted as a function of reflected radiation difference between point *a* and *b*. Labels from A to F identify the instrument type.

Table 1. Selected air temperature measurement instruments and their main characteristics.

Instrument ID	Sensor type	Resolution (°C)	Shield type	Note on shield
Type A	Pt100	0.012	Fan aspirated	"spheroidal" type
Type B	Pt100	0.003	Passive	"classical" type
Type C	Thermo hygrometer	0.001	Passive helicoidal	"short" type
Type D	Thermo hygrometer	0.001	Passive helicoidal	"long" type
Type E	Pt100	0.01	Passive	"cylinder" type
Type F	Pt100	0.01	Passive	"classical" type

Table 2. Sensors used for measuring the quantities of influence and their positioning referenced to the scheme of Figure 1.

Quantity	Sensor type	positioning (see Fig. 1)
Temperature and Relative Humidity	Pt100 class A and capacitor (thermo-hygrometer)	Central point
Wind	Cups and vane	Central point
Global incident Radiation	Thermopile (pyranometer)	Point *a*, facing up
Global reflected Radiation	Thermopile (pyranometer)	Point *a*, facing down
Global incident Radiation	Thermopile (pyranometer)	Point *b*, facing up
Global reflected Radiation	Thermopile (pyranometer)	Point *b*, facing down

645

Table 3. Results of the evaluation of Δt_{instr} and the associated uncertainties $u_{\Delta t_{instr}}$ for each instrument type.

Sensor type	Type A (°C)	Type B (°C)	Type C (°C)	Type D (°C)	Type E (°C)	Type F (°C)
Δt_{instr}	0.12	-0.47	0.022	0.002	0.043	0.063
$u_{\Delta t_{instr}}$	0.05	0.09	0.015	0.026	0.035	0.067

Table 4. Results of the evaluation of Δt_{site} and the associated uncertainties $u_{\Delta t_{site}}$ for each instrument type.

Sensor type	Type A (°C)	Type B (°C)	Type C (°C)	Type D (°C)	Type E (°C)	Type F (°C)

Δt_{site}	0.02	0.17	0.12	0.10	0.08	0.11
$u_{\Delta t_{site}}$	0.02	0.17	0.11	0.11	0.09	0.09

Table 5. Contributions to the uncertainty budget evaluated in the laboratory and on-field characterization.

	Type A (°C)	**Type B (°C)**	**Type C (°C)**	**Type D (°C)**	**Type E (°C)**	**Type F (°C)**
u_{res}	0.004	0.001	3e-4	3e-4	0.003	0.003
u_{lab}	0.01	0.01	0.01	0.01	0.01	0.01
$u_{\Delta t_{instr}}$	0.05	0.09	0.015	0.026	0.035	0.067
$u_{\Delta t_{site}}$	0.02	0.17	0.11	0.11	0.09	0.09
$u_{\Delta t_{air}}$	0.05	0.19	0.11	0.11	0.10	0.11
$\boldsymbol{U_{\Delta t_{air}}}$ (k = 2)	**0.11**	**0.38**	**0.22**	**0.23**	**0.20**	**0.23**

Table 6. Maximum difference - Δt_{air} - measured, for each manufacturer on a significant number of events and with the associated uncertainty from Table 5. Values are rounded at first decimal and $U_{\Delta t_{air}}$ rounded up according to normative (EA-4/02).

Instrument Type	**Max diff Δt_{air} (°C)**	$U_{\Delta t_{air}}$ $\boldsymbol{U_{\Delta t_{air}}}$ **(°C) (k = 2)**
A	1.4	0.1
B	3.1	0.4
C	1.4	0.3

D	1.2	0.3
E	1.9	0.2
F	3.8	0.3